

Carbon Dioxide Reduction

A Monolithically Integrated Gallium Nitride Nanowire/Silicon Solar Cell Photocathode for Selective Carbon Dioxide Reduction to Methane

Yichen Wang, Shizhao Fan, Bandar AlOtaibi, Yongjie Wang, Lu Li, and Zetian Mi*^[a]

Abstract: A gallium nitride nanowire/silicon solar cell photocathode for the photoreduction of carbon dioxide (CO₂) is demonstrated. Such a monolithically integrated nanowire/solar cell photocathode offers several unique advantages, including the absorption of a large part of the solar spectrum and highly efficient carrier extraction. With the incorporation of copper as the co-catalyst, the devices exhibit a Faradaic efficiency of about 19% for the 8e⁻ photoreduction to CH₄ at -1.4 V vs Ag/AgCl, a value that is more than thirty times higher than that for the 2e⁻ reduced CO (ca. 0.6%).

With the increased fossil fuel consumption, the level of atmospheric CO₂ has shown a steady increase during the past decades. In this regard, the conversion of CO₂ into hydrocarbon fuel via solar-powered photocatalysis or photoelectrocatalysis (PEC) approach has been intensively studied, as it can simultaneously decrease the amount of CO₂ in atmosphere and reduce the use of conventional fossil fuel.^[1] Compared to photocatalysis, a PEC system offers several important advantages, including efficient charge carrier separation and collection of the oxidation and reduction products at the anodic and cathodic electrode, respectively. Various photocathodes, including Si, GaP, CuInS₂, CuO/Fe₂O₃, InP, and ZnTe have been developed for the reduction of CO₂.^[2] Their performance, however, has remained very limited, owing the poor light absorption and/or rapid corrosion and degradation. Moreover, much of the work has been focused on the conversion of CO₂ into the 2e⁻ reduced species such as carbon monoxide (CO), and the 8e⁻ photoreduction of CO₂ to methane (CH₄) has remained extremely challenging, which is due to the kinetic barriers associated with the multiple proton coupled electron transfer (PCET) process.^[1b,3] Recently, the use of metal nitrides, including Ga(In)N, for CO₂ reduction has attracted considerable attention.^[4] Compared to conventional metal oxides, Ga(In)N possesses several unique advantages, including tunable energy bandgap across nearly the entire solar spectrum, thermody-

namically favorable conduction band edge position to reduce CO₂ to various hydrocarbons, and superior charge carrier transport properties.^[5] Moreover, owing to the ionic bonding character and the absence of surface states in the middle of the bandgap, Ga(In)N is much more stable compared to other III-V compound semiconductors.^[5g,6] The surface recombination velocity (ca. 10⁴ cm s⁻¹) is also smaller than other III-V materials.

In this context, Yotsuhashi et al. have studied the reduction of CO₂ using planar GaN photocathodes grown on sapphire substrate.^[4b-e] More recently, significantly enhanced photocatalytic activities have been demonstrated with the use of Ga(In)N nanowire photocatalysts and photoelectrodes.^[6,7] Such nanostructured photoelectrodes can exhibit enhanced light absorption and carrier extraction efficiency, which is due to the large surface-to-volume ratios. Moreover, the spacing amongst nanowires can facilitate the diffusion of electrolyte and improve the photoelectrocatalytic performance.^[5g,8] Nearly defect-free Ga(In)N nanowire photoelectrodes can also be readily grown on foreign substrates, including Si and SiO₂,^[9] thereby making it possible for the direct integration with Si solar cell technology. Such monolithically integrated nanowire/Si solar cell photocathodes can offer significantly enhanced efficiency, greatly reduced cost, and scalable manufacturing compared to previously reported devices. To date, however, the use of a metal nitride nanowire photocathode for CO₂ reduction has not been reported.

Herein, we report on the first demonstration of a metal nitride nanowire/Si solar cell photocathode for the reduction of CO₂ under simulated sunlight illumination. Unique to such a monolithically integrated photocathode is that the Si solar cell substrate can harvest a large part of the solar spectrum and the GaN nanowires can significantly enhance the extraction of photo-generated electrons. With the incorporation of Cu co-catalyst on GaN nanowire arrays, we have measured the direct conversion of CO₂ into CH₄ and CO. At -1.4 V vs Ag/AgCl, the Faradaic efficiency can reach about 19% for the 8e⁻ photoreduction to CH₄, which is more than 30 times higher than that for the 2e⁻ reduced CO (ca. 0.6%). Detailed studies further suggest the synergistic effect of GaN nanowires and Cu co-catalyst in significantly enhancing the selectivity for the photoreduction of CO₂ to CH₄. The GaN nanowire/Si solar cell photocathode also showed excellent stability towards CO₂ reduction.

The photocathode (Figure 1a) consists of a planar n⁺-p Si solar cell wafer and n-GaN nanowire arrays. The Si solar cell functions as both the substrate and the photon absorber. It

[a] Dr. Y. Wang, S. Fan, B. AlOtaibi, Y. Wang, Dr. L. Li, Prof. Z. Mi
Department of Electrical and Computer Engineering, McGill University
3480 University Street, Montreal, QC H3A 0E9 (Canada)
E-mail: zetian.mi@mcgill.ca

Supporting information for this article can be found under:
<http://dx.doi.org/10.1002/chem.201601642>.

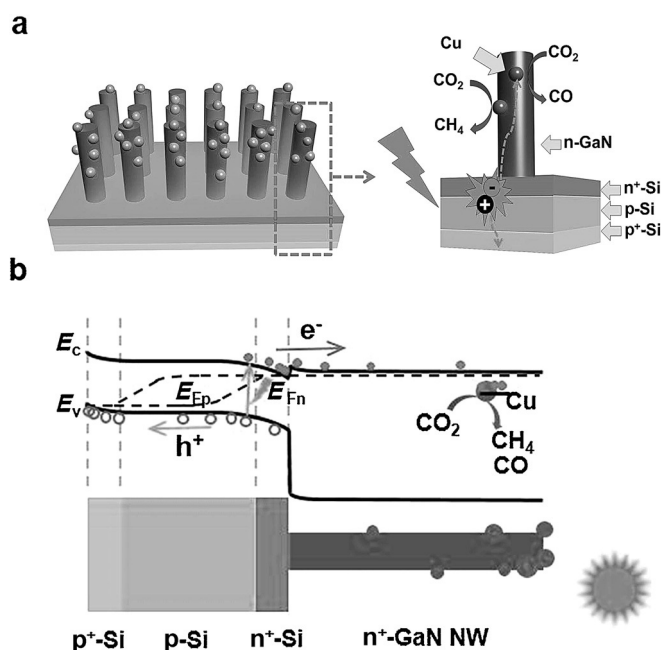


Figure 1. a) A representation of the Cu/GaN/n⁺-p Si photocathode and b) the energy band diagram of the GaN nanowire/Si solar cell photocathode under illumination.

was prepared by a two-step method including the deposition of phosphorus and boron as the n-type and p-type dopants on the front and back sides of the p-type wafer by spin-coating, respectively, and the subsequent annealing under a N₂ atmosphere at 900 °C for 4 h (see the Supporting Information).^[10] GaN nanowire arrays were then grown on the n-type surface of the Si solar cell wafer by plasma-assisted molecular beam epitaxy (PA-MBE) under nitrogen-rich conditions. Ge was incorporated as n-type dopant.^[11] Previous studies have shown that Cu can deliver a range of reaction products such as CO and CH₄, owing to its medium hydrogen overpotential.^[12] There-

fore, Cu nanoparticles were formed with the photodeposition method as the co-catalyst (see the Supporting Information).

Figure 1 b shows the energy band diagram of the monolithically integrated GaN nanowire/Si solar cell photocathode under illumination. In this design, the solar cell can effectively absorb photons with wavelengths < 1.1 μm, while photogenerated electrons in the solar cell can be readily injected into the n-GaN nanowires, owing to the small offset between the GaN and Si conduction band edges and the heavy n-type doping.^[13] Moreover, the GaN nanowires are doped heavily as n-type, which significantly reduces the surface depletion width associated with the upward band bending. Under illumination, the upshifting of the quasi-electron Fermi level further reduces the upward surface band bending. The abundance of photoexcited electrons ensures nearly flat-band conditions in the GaN nanowire. Therefore, the photoexcited electrons can readily reach the Cu nanoparticles to facilitate the catalytic reaction, considering a higher electron affinity of Cu compared to GaN.^[10]

Figure 2a shows the scanning electron microscopy (SEM) image of GaN nanowires on Si solar cell with the incorporation Cu particles. The nanowires are vertically aligned on the Si solar cell, with lengths and diameters in the ranges of 100 nm and 30–40 nm, respectively. It is noted that some Cu particles are formed directly on the top and lateral surfaces of the nanowires. Detailed structural characterization of the GaN nanowire/Cu photocatalyst was further performed using transmission electron microscopy (TEM; Figure 2b). The presence of Cu based particles on the lateral surface of GaN nanowires is evident, and the sizes vary in the range between 10 and 30 nm. Some Cu particles aggregate to form clusters with sizes in the range of 50 to 100 nm. The presence of Cu particles (area A) on GaN nanowires (area B) is also supported by detailed energy-dispersive X-ray spectroscopy (EDX) studies (Supporting Information, Section 4). X-ray photoelectron spectroscopy (XPS) and Auger Cu LMM spectroscopy measurements were further

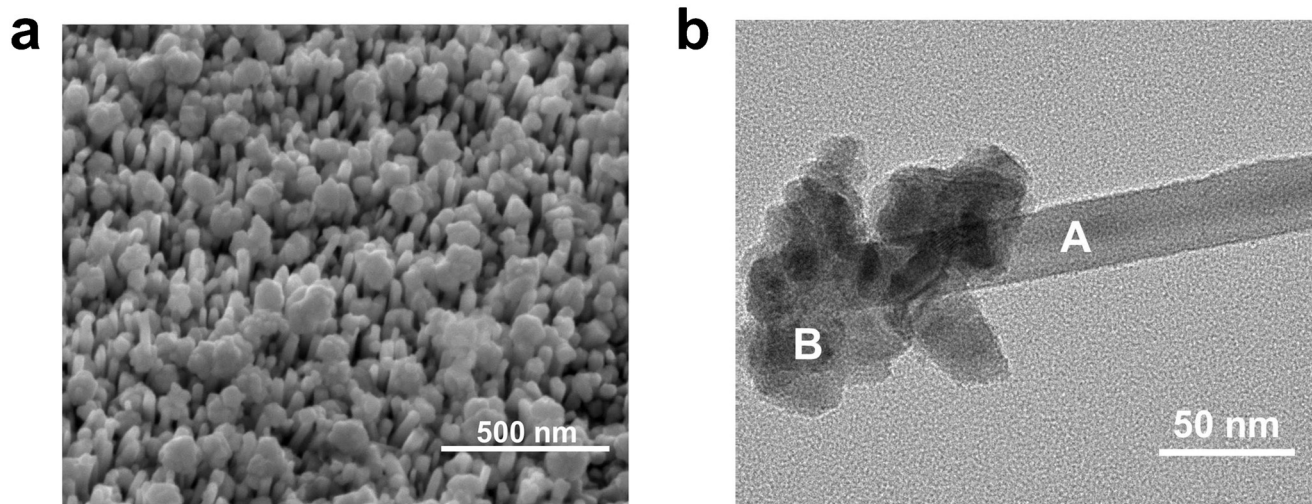


Figure 2. a) SEM images of Cu/GaN/n⁺-p Si and b) TEM image of GaN nanowires with the incorporation of Cu particles (A and B indicate the areas which are tested by EDX shown in the Supporting Information).

performed to probe the chemical status of Cu element formed on Cu/GaN/n⁺-p Si. It was confirmed the primary presence of Cu element on the GaN nanowire/Si solar cell photocathode is metallic Cu (Supporting Information, Section 5).

The PEC performance of CO₂ reduction was first investigated by linear sweep voltammetry (LSV). Figure 3a shows the LSV curves of the GaN/n⁺-p Si solar cell devices with and without the incorporation of Cu co-catalyst under dark and illumination conditions at a scan rate of 20 mVs⁻¹. The LSV curve for a Si

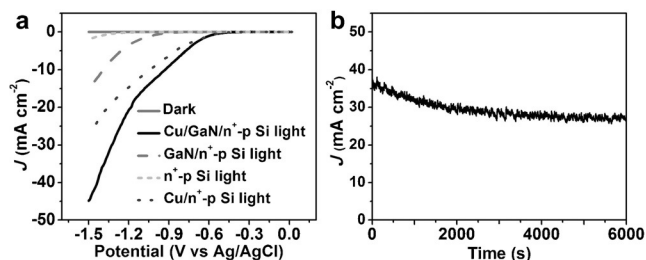


Figure 3. a) Linear sweep voltammetry of different photocathodes with a Pt counter electrode (vs Ag/AgCl) at a scan rate of 20 mVs⁻¹ in 0.5 M KHCO₃ (pH ca. 8). b) Chronoamperometric curves of Cu/GaN/n⁺-p Si photocathode with a Pt counter electrode at -1.4 V (vs Ag/AgCl) in 0.5 M KHCO₃ (pH ca. 8).

solar cell with and without the incorporation of Cu is also shown for comparison. Under dark conditions, there are negligible currents for all the samples in the potential range from 0 V to -1.5 V (solid gray curve). A 300 W Xenon lamp (Excelitas Technologies) was used as the illumination source. Under illumination, various photocurrent levels were measured for the different samples. Shown in Figure 3a, the photocurrent for a Si solar cell photocathode (short dash light gray curve) without any co-catalyst is about 1.95 mAcm⁻² at -1.5 V vs Ag/AgCl. The very low photocurrent is due to the inefficient carrier extraction from a planar Si surface without any co-catalysts. With the use of GaN nanowires or Cu co-catalysts, significantly improved photocurrent and onset potential were measured, shown as the dashed gray and dotted dark gray curves in Figure 3a, respectively, owing to the enhanced carrier extraction. The best result is obtained for the Cu/GaN/n⁺-p Si device, wherein both Cu co-catalyst and GaN nanowires are integrated with the Si solar cell. The photocurrent density is 44.9 mA cm⁻² at -1.5 V (solid black curve), with an onset potential of -0.43 V. These results indicate the important roles of n-GaN nanowire and Cu co-catalyst for catalyzing the reduction reaction. The stability of the nanowire photocathode is further investigated by the chronoamperometry test. Figure 3b shows the current-time curve measured at a constant voltage of -1.4 V vs. Ag/AgCl for Cu/GaN/n⁺-p Si. It is seen that the current shows a small reduction with time. In 6000 s, the photocurrent loss is about 30%. Interestingly, most of the current loss occurred during the initial part of the measurement, and the photocurrent becomes highly stable afterwards, with only about 6% decrease per hour, indicating very stable performance. The slow attenuation could be related to the etching of the n-GaN/n-Si interface.^[10]

To gain further insight into the photoelectrocatalytic activity of the GaN nanowire photocathode for CO₂ reduction, we analyzed the reaction products in the cathode after 6000 s chronoamperometric measurements at different potentials from -1.1 V to -1.5 V vs Ag/AgCl. The flame ionization detector (FID) attached to the gas chromatograph (Shimadzu GC-2014) was used to detect CH₄ and CO, and the thermal conductivity detector (TCD) attached to the gas chromatograph (Shimadzu GC-8A) was employed to measure H₂. Figure 4a shows the reduction products, including CH₄ and CO generated in the Cu/GaN/n⁺-p Si photocathode measured at different potentials. It is seen that the rate of CH₄ production is increased dramatically from about 1.21 μmolh⁻¹cm⁻² at -1.1 V to about 25.5 μmolh⁻¹cm⁻² at -1.4 V. The rate of CO generation, however, shows a decreasing trend by applying a more negative potential.

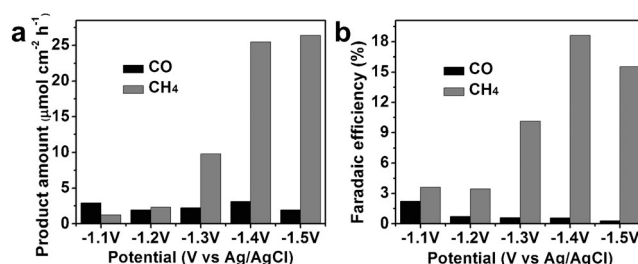


Figure 4. a) The amount of reaction products of Cu/GaN/n⁺-p Si, including CO and CH₄, measured in 6000 s at different potentials from -1.1 V to -1.5 V (vs Ag/AgCl) in 0.5 M KHCO₃ (pH ca. 8). b) The measured Faradaic efficiency of the Cu/GaN/n⁺-p Si photocathode for different reaction products at different potentials from -1.1 V to -1.5 V (vs. Ag/AgCl) in 0.5 M KHCO₃ (pH ca. 8).

One of the primary challenges for PEC CO₂ reduction is the selectivity of reduction products towards CO₂ conversion, which is further complicated by the competition from H₂ generation in the cathode.^[14] Faradaic efficiency is the value that not only shows the total conversion efficiency from electrical energy to chemical energy, but also exhibits a distribution for all the reduction products in the cathode side. Figure 4b shows the Faradaic efficiency for CH₄ and CO generation in the Cu/GaN/n⁺-p Si cathode after 6000 s chronoamperometric measurements at different potentials from -1.1 V to -1.5 V vs Ag/AgCl. The Faradaic efficiencies for all the products, including CH₄, CO, and H₂ are shown in the Supporting Information, Table S1. It is seen that the Faradaic efficiency of the 2e⁻ reduced CO shows a declining trend, while the Faradaic efficiency of the 8e⁻ reduced CH₄ increases drastically with increasingly more negative potential. At -1.4 V, the Faradaic efficiency of CH₄ production is about 19%, which is more than 30 times higher than that of CO generation (ca. 0.6%). The measured Faradaic efficiency of CH₄ production is also much higher than previously reported values.^[2c,15] The significantly increased selectivity for CH₄ production is directly related to the enhanced multiple proton coupled electron transfer (PCET) process, which is due to the relatively large negative potential associated with the conduction bandedge of GaN nanowires and the

use of Cu co-catalyst. In the process of CH₄ generation, CO is also consumed.^[1h, 16]

To shed light on the synergistic effect of GaN nanowires and Cu cocatalyst, the Faradaic efficiencies for CO₂ reduction are compared for the Cu/GaN/n⁺-p Si, GaN/n⁺-p Si, Cu/n⁺-p Si, and n⁺-p Si photocathodes. Shown in Figure 5, it is seen that the use of Cu particles is essential for CH₄ generation. This is in

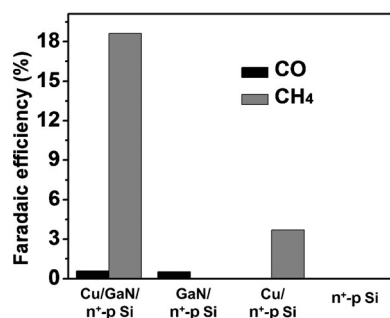


Figure 5. The measured Faradaic efficiency of products for different samples at -1.4 V (vs Ag/AgCl) in 0.5 M KHCO₃ (pH ca. 8).

agreement with previous reports that copper is a suitable material because it can catalyze CO₂ reduction to a range of products such as CH₄ and CO with medium overpotential towards hydrogen evolution reaction and weak CO adsorption, which can lead to the C–O bonds breaking.^[4b, 12c] However, with the use Cu of catalyst but without GaN nanowire arrays, the Faradic efficiency of CH₄ generation is only about 3.7%. The significant enhancement in the Faradic efficiency of CH₄ generation for the Cu/GaN/n⁺-p Si photocathode, compared to the sample without GaN nanowires, is attributed to the extremely efficient carrier extraction and the highly reactive GaN nonpolar lateral surfaces for CO₂ adsorption and dissociation.^[4a]

In summary, we have demonstrated, for the first time, metal nitride nanowire photocathodes for PEC reduction of CO₂. The GaN nanowires are integrated with a standard Si solar cell, which offers several unique advantages for CO₂ reduction, including the absorption of a large part of the solar spectrum, highly efficient carrier extraction, and highly selective CH₄ production. Moreover, the Faradaic efficiency for CH₄ production can be tuned to be more than 30 times higher than that for CO generation. Such a monolithically integrated GaN nanowire/Si solar cell photocathode provides a promising approach for the scalable manufacturing of high efficiency and low cost PEC devices and systems for the selective reduction of CO₂ under direct sunlight irradiation.

Acknowledgements

This work was supported by the by the Natural Sciences and Engineering Research Council of Canada (NSERC) and the Climate Change and Emissions Management Corporation (CCEMC).

Keywords: carbon dioxide reduction • gallium nitride • photocathodes • photoelectrocatalysis • solar fuel

- a) A. Bachmeier, S. Hall, S. W. Ragsdale, F. A. Armstrong, *J. Am. Chem. Soc.* **2014**, *136*, 13518–13521; b) J. Bonin, M. Robert, M. Routier, *J. Am. Chem. Soc.* **2014**, *136*, 16768–16771; c) J. Etedgui, Y. Diskin-Posner, L. Weiner, R. Neumann, *J. Am. Chem. Soc.* **2011**, *133*, 188–190; d) S. N. Habisreutinger, L. Schmidt-Mende, J. K. Stolarczyk, S. N. Habisreutinger, L. Schmidt-Mende, J. K. Stolarczyk, *Angew. Chem. Int. Ed.* **2013**, *52*, 7372–7408; *Angew. Chem.* **2013**, *125*, 7516–7557; e) J. Rongé, T. Bosserez, D. Martel, C. Nervi, L. Boarino, F. Taulelle, G. Decher, S. Bordiga, J. A. Martens, *Chem. Soc. Rev.* **2014**, *43*, 7963–7981; f) T. Inoue, A. Fujishima, S. Konishi, K. Honda, *Nature* **1979**, *277*, 637–638; g) K. R. Thampi, J. Kiwi, M. Gratzel, *Nature* **1987**, *327*, 506–508; h) B. Kumar, M. Llorente, J. Froehlich, T. Dang, A. Sathrum, C. P. Kubiak, *Annu. Rev. Phys. Chem.* **2012**, *63*, 541–569.
- a) E. E. Barton, D. M. Rampulla, A. B. Bocarsly, *J. Am. Chem. Soc.* **2008**, *130*, 6342–6344; b) M. Halmann, *Nature* **1978**, *275*, 115–116; c) P. Li, H. Wang, J. Xu, H. Jing, J. Zhang, H. Han, F. Lu, *Nanoscale* **2013**, *5*, 11748–11754; d) L. Junfu, C. Baozhu, *J. Electroanal. Chem.* **1992**, *324*, 191–200; e) T. J. LaTempa, S. Rani, N. Bao, C. A. Grimes, *Nanoscale* **2012**, *4*, 2245–2250; f) J. Qiu, G. Zeng, M.-A. Ha, M. Ge, Y. Lin, M. Hettick, B. Hou, A. N. Alexandrova, A. Javey, S. B. Cronin, *Nano Lett.* **2015**, *15*, 6177–6181; g) J.-W. Jang, S. Cho, G. Magesh, Y. J. Jang, J. Y. Kim, W. Y. Kim, J. K. Seo, S. Kim, K.-H. Lee, J. S. Lee, *Angew. Chem. Int. Ed.* **2014**, *53*, 5852–5857; *Angew. Chem.* **2014**, *126*, 5962–5967.
- a) J. L. White, M. F. Baruch, J. E. Pander Iii, Y. Hu, I. C. Fortmeyer, J. E. Park, T. Zhang, K. Liao, J. Gu, Y. Yan, T. W. Shaw, E. Abelev, A. B. Bocarsly, *Chem. Rev.* **2015**, *115*, 12888–12935; b) R. Hinogami, Y. Nakamura, S. Yae, Y. Nakato, *J. Phys. Chem. B* **1998**, *102*, 974–980; c) R. Hinogami, T. Mori, S. Yae, Y. Nakato, *Chem. Lett.* **1994**, 1725–1728.
- a) B. AlOtaibi, S. Fan, D. Wang, J. Ye, Z. Mi, *ACS Catal.* **2015**, *5*, 5342–5348; b) S. Yotsuhashi, M. Deguchi, Y. Zenitani, R. Hinogami, H. Hashiba, Y. Yamada, K. Ohkawa, *Appl. Phys. Express* **2011**, *4*, 117101; c) S. Yotsuhashi, M. Deguchi, H. Hashiba, Y. Zenitani, R. Hinogami, Y. Yamada, K. Ohkawa, *Appl. Phys. Lett.* **2012**, *100*, 243904; d) S. Yotsuhashi, M. Deguchi, Y. Zenitani, R. Hinogami, H. Hashiba, Y. Yamada, K. Ohkawa, *Jpn. J. Appl. Phys.* **2012**, *51*, 02BP07; e) S. Yotsuhashi, M. Deguchi, Y. Yamada, K. Ohkawa, *AIP Advances* **2014**, *4*, 067135.
- a) K. Aryal, B. N. Pantha, J. Li, J. Y. Lin, H. X. Jiang, *Appl. Phys. Lett.* **2010**, *96*, 052110; b) J.-S. Hwang, T.-Y. Liu, S. Chattopadhyay, G.-M. Hsu, A. M. Basilio, H.-W. Chen, Y.-K. Hsu, W.-H. Tu, Y.-G. Lin, K.-H. Chen, C.-C. Li, S.-B. Wang, H.-Y. Chen, L.-C. Chen, *Nanotechnology* **2013**, *24*, 055401; c) W.-H. Tu, Y.-K. Hsu, C.-H. Yen, C.-I. Wu, J.-S. Hwang, L.-C. Chen, K.-H. Chen, *Electrochem. Commun.* **2011**, *13*, 530–533; d) D.-H. Tu, H.-C. Wang, P.-S. Wang, W.-C. Cheng, K.-H. Chen, C.-I. Wu, S. Chattopadhyay, L.-C. Chen, *Int. J. Hydrogen Energy* **2013**, *38*, 14433–14439; e) P. D. Tran, L. H. Wong, J. Barber, J. S. C. Loo, *Energy Environ. Sci.* **2012**, *5*, 5902–5918; f) H. S. Jung, Y. J. Hong, Y. Li, J. Cho, Y.-J. Kim, G.-C. Yi, *ACS Nano* **2008**, *2*, 637–642; g) D. Wang, A. Pierre, M. G. Kibria, K. Cui, X. Han, K. H. Bevan, H. Guo, S. Paradis, A.-R. Hakima, Z. Mi, *Nano Lett.* **2011**, *11*, 2353–2357; h) S. Schäfer, S. A. Wyrzgol, R. Caterino, A. Jentys, S. J. Schoell, M. Hävecker, A. Knop-Gericke, J. A. Lercher, I. D. Sharp, M. Stutzmann, *J. Am. Chem. Soc.* **2012**, *134*, 12528–12535; i) L. Caccamo, J. Hartmann, C. Fàbrega, S. Estradé, G. Lillenkamp, J. D. Prades, M. W. G. Hoffmann, J. Ledig, A. Wagner, X. Wang, L. Lopez-Conesa, F. Peiró, J. M. Rebled, H.-H. Wehmann, W. Daum, H. Shen, A. Waag, *ACS Appl. Mater. Interfaces* **2014**, *6*, 2235–2240; j) M. G. Kibria, F. A. Chowdhury, S. Zhao, B. AlOtaibi, M. L. Trudeau, H. Guo, Z. Mi, *Nat. Commun.* **2015**, *6*, 6797; k) K. Maeda, K. Domen, *J. Phys. Chem. C* **2007**, *111*, 7851–7861.
- B. AlOtaibi, H. P. T. Nguyen, S. Zhao, M. G. Kibria, S. Fan, Z. Mi, *Nano Lett.* **2013**, *13*, 4356–4361.
- a) M. G. Kibria, H. P. T. Nguyen, K. Cui, S. Zhao, D. Liu, H. Guo, M. L. Trudeau, S. Paradis, A.-R. Hakima, Z. Mi, *ACS Nano* **2013**, *7*, 7886–7893; b) L. Li, S. Fan, X. Mu, Z. Mi, C.-J. Li, *J. Am. Chem. Soc.* **2014**, *136*, 7793–7796.
- E. Garnett, P. Yang, *Nano Lett.* **2010**, *10*, 1082–1087.
- S. Zhao, M. G. Kibria, Q. Wang, H. P. T. Nguyen, Z. Mi, *Nanoscale* **2013**, *5*, 5283–5287.

- [10] S. Fan, B. AlOtaibi, S. Y. Woo, Y. Wang, G. A. Botton, Z. Mi, *Nano Lett.* **2015**, *15*, 2721–2726.
- [11] J. Schörmann, P. Hille, M. Schäfer, J. Müßener, P. Becker, P. J. Klar, M. Kleine-Boymann, M. Rohnke, M. de La Mata, J. Arbiol, D. M. Hofmann, J. Teubert, M. Eickhoff, *J. Appl. Phys.* **2013**, *114*, 103505.
- [12] a) Y. Hori, K. Kikuchi, S. Suzuki, *Chem. Lett.* **1985**, 1695–1698; b) M. Jitaru, D. A. Lowy, M. Toma, B. C. Toma, L. Oniciu, *J. Appl. Electrochem.* **1997**, *27*, 875–889; c) G. Magesh, E. S. Kim, H. J. Kang, M. Banu, J. Y. Kim, J. H. Kim, J. S. Lee, *J. Mater. Chem. A* **2014**, *2*, 2044–2049.
- [13] S. Guha, N. A. Bojarczuk, *Appl. Phys. Lett.* **1998**, *72*, 415–417.
- [14] J. Qiao, Y. Liu, F. Hong, J. Zhang, *Chem. Soc. Rev.* **2014**, *43*, 631–675.
- [15] J. Cheng, M. Zhang, G. Wu, X. Wang, J. Zhou, K. Cen, *Environ. Sci. Technol.* **2014**, *48*, 7076–7084.
- [16] a) Y. Hori, A. Murata, R. Takahashi, S. Suzuki, *J. Am. Chem. Soc.* **1987**, *109*, 5022–5023; b) Y. Hori, A. Murata, R. Takahashi, *J. Chem. Soc. Faraday Trans. 1* **1989**, *85*, 2309–2326.

Received: April 8, 2016

Published online on May 24, 2016